Collapse of the low temperature insulating state in Cr-doped V_2O_3 thin films

P. Homm, L. Dillemans, M. Menghini, B. Van Bilzen, P. Bakalov, C.-Y. Su, R. Lieten, M. Houssa, D. Nasr Esfahani, L. Covaci, F. M. Peeters, J. W. Seo, and J.-P. Locquet

Citation: Appl. Phys. Lett. **107**, 111904 (2015);
View online: https://doi.org/10.1063/1.4931372
View Table of Contents: http://aip.scitation.org/toc/apl/107/11
Published by the American Institute of Physics

Collapse of the low temperature insulating state in Cr-doped V_2O_3 thin films

P. Homm,[1,a)] L. Dillemans,[1] M. Menghini,[1] B. Van Bilzen,[1] P. Bakalov,[1] C.-Y. Su,[1] R. Lieten,[1] M. Houssa,[1] D. Nasr Esfahani,[2] L. Covaci,[2] F. M. Peeters,[2] J. W. Seo,[3] and J.-P. Locquet[1]
[1]*Department of Physics and Astronomy, KU Leuven, Celestijnenlaan 200D, 3001 Leuven, Belgium*
[2]*Department of Physics, University of Antwerp, Groenenborgerlaan 171, B-2020 Antwerp, Belgium*
[3]*Department of Materials Engineering, KU Leuven, Kasteelpark Arenberg 44, 3001 Leuven, Belgium*

(Received 12 June 2015; accepted 6 September 2015; published online 18 September 2015; publisher error corrected 22 September 2015)

We have grown epitaxial Cr-doped V_2O_3 thin films with Cr concentrations between 0% and 20% on (0001)-Al_2O_3 by oxygen-assisted molecular beam epitaxy. For the highly doped samples (>3%), a regular and monotonous increase of the resistance with decreasing temperature is measured. Strikingly, in the low doping samples (between 1% and 3%), a collapse of the insulating state is observed with a reduction of the low temperature resistivity by up to 5 orders of magnitude. A vacuum annealing at high temperature of the films recovers the low temperature insulating state for doping levels below 3% and increases the room temperature resistivity towards the values of Cr-doped V_2O_3 single crystals. It is well-know that oxygen excess stabilizes a metallic state in V_2O_3 single crystals. Hence, we propose that Cr doping promotes oxygen excess in our films during deposition, leading to the collapse of the low temperature insulating state at low Cr concentrations. These results suggest that slightly Cr-doped V_2O_3 films can be interesting candidates for field effect devices. © *2015 AIP Publishing LLC*. [http://dx.doi.org/10.1063/1.4931372]

The metal-insulator transition (MIT) in vanadium oxides forms a topic of intense research since many years. Not only are there many different structural phases present in the V-O phase diagram[1] but also a large distribution of MIT temperatures is observed.[2] Most well-known phases are vanadium sesquioxide (V_2O_3) and vanadium dioxide (VO_2) with transition temperatures of 160 K and 340 K and a change in resistivity across the MIT of about seven and four orders of magnitude, respectively.[3,4] Because of this large change in resistivity, there has been considerable interest to drive this transition with additional stimuli besides the change in temperature.[5] Most relevant would be to induce the transition through the application of an electric field as in a field-effect transistor (FET) device. Electric field induced resistive switching has been observed many times but so far this has been mostly limited to either: (i) only a small change of the maximal resistivity, (ii) local temperature changes induced by Joule heating, (iii) changes in the oxygen content, and (iv) the formation of locally more conducting paths.[6–10] Essentially, it has turned out that the correlated electron states in these oxides are rather stable and can not easily be changed through the application of an electric field.

Our ultimate research goal is to find a method to tune the properties of vanadium oxide based compounds in order to facilitate the electric field induced MIT. One of these methods is to change the dimensionality towards 2D systems by using epitaxially grown thin films (TF). In that case, the lattice parameters of the film tend to change and adapt to those of the single crystalline substrates with the electrical properties being modified as demonstrated in TF grown with different methods.[11–16] One other well-known method is to dope the oxide with different elements such as Cr and Ti. For the case of Cr doping, Frenkel *et al.*[17] have shown evidence in single crystals (SC) that Cr atoms create substitutional strain defects in the V_2O_3 lattice, leading to a disordered system of bonds around the average trigonal lattice determined by X-ray diffraction (XRD). The long range strain field around Cr atoms results in insulating regions even at the low Cr concentration of 1%. In particular, for Cr concentrations below 1.8% besides the low temperature (LT) MIT, a paramagnetic metal (PM) to paramagnetic insulator (PI) transition around room temperature has been reported in bulk.[3] When increasing dopant concentration, a transition from an antiferromagnet insulator (AFI) to a PI takes place at low temperatures. In this case, both the low temperature resistivity (LTR) and the room temperature resistivity (RTR) increase considerably as observed in single crystal[18–20] and thin film alloys.[21] Another effective way to manipulate the MIT is the non-stoichiometry, which in the literature has been formulated as $V_2O_{3+\delta}$ or $V_{2-y}O_3$, since metal vacancies can be generated in the cation sublattice due to the filling of all the available oxygen sites. For that case, it is well-known that the electrical properties change drastically with increased oxygen doping and that beyond $\delta = 0.03$ the LT MIT is suppressed.[22–24] This stabilization of the metallic phase at all temperatures has also been observed with Ti doping and application of hydrostatic pressure[24] and in Cr-doped nonstoichiometric V_2O_3 SC as reported in Ref. 25 for 1% Cr concentration and around 0.04 oxygen excess.

In this work, we report the epitaxial growth of Cr-doped V_2O_3 TF on Al_2O_3 substrates using molecular beam epitaxy (MBE), and we compare their structural properties (*a* and *c* lattice parameters) with those of the bulk compounds. Next, the electrical properties are reported with the striking result that the low Cr-doped films show a nearly metallic behavior at all temperatures. To elucidate the main reason for this observation, vacuum annealing at high temperature is performed on

a)Pia.Homm@fys.kuleuven.be

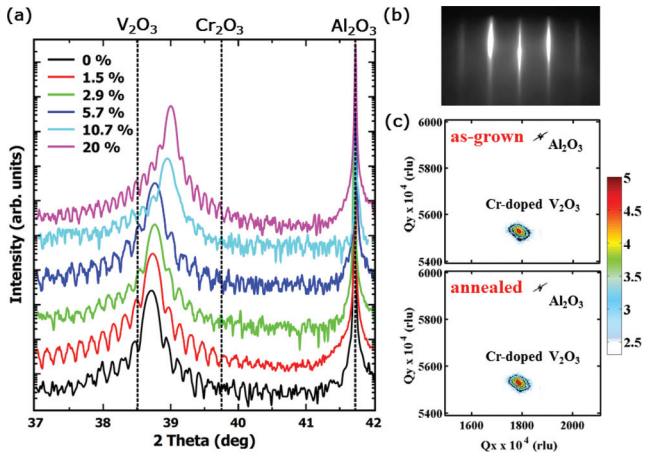

FIG. 1. (a) XRD $\vartheta/2\vartheta$ scans around the (0006) reflection of Cr-doped V_2O_3 TF showing Pendellösung fringes. (b) RHEED image taken after deposition along the [10$\bar{1}$0] direction of the undoped sample. (c) RSMs of the (1 0 $\bar{1}$ $\underline{10}$) substrate and layer peaks for the 1.5% Cr-doped sample before and after annealing. Qx and Qy are the components of the scattering vector along in- and out-of-plane directions, respectively. The intensity scale is logarithmic.

the films, which results in a recovery of the LT insulating state for the low Cr-doped cases.

The Cr-doped V_2O_3 TF (60 to 80 nm) have been deposited by oxygen-assisted MBE in a vacuum chamber (Riber) with a base pressure of 10^{-9} mbar. Substrates of (0001)-Al_2O_3 were used without prior cleaning and were slowly heated to the growth temperature of 650 °C as measured with a thermocouple. Alloys with Cr concentrations between 0% and 20% have been grown by co-deposition of V and Cr metals in an O_2 partial pressure of $8.2–8.5 \times 10^{-6}$ Torr, which constitutes most of the total pressure in the chamber and is at least two orders of magnitude higher than residual gases like H_2. V was evaporated from an electron gun with a deposition rate of 0.1 Å/s calibrated with a quartz crystal microbalance (QCM) prior deposition, while Cr was evaporated from a Knudsen cell (Veeco) by using different Cr fluxes to obtain the particular Cr/V ratios. Very low deposition rates were achieved by extrapolating calibration rate curves fitted with an exponential temperature-dependence. The growth time is 60 min for all samples. During growth, the metal layers will combine with the O_2 producing the oxide layers. This will translate in a final oxide layer thicker than expected from considering only the V + Cr deposition rates. As a result, the thickness of the samples increases more than 20% for the highest Cr concentration. *In situ* reflection high energy electron diffraction (RHEED) is used qualitatively to confirm the epitaxy. After deposition, the samples were characterized by means of high resolution XRD, X-ray reflectivity (XRR), and X-ray reciprocal space mapping (RSM) using a Panalytical X'pert Pro diffractometer. Temperature dependent resistivity measurements were assessed in the Van der Pauw (VDP) configuration with Au/Cr contacts and using an Oxford Optistat CF2-V cryostat with a sweep rate of 1.5 K per minute. After their initial electrical characterization, the TF were annealed in vacuum for 5 min at the same temperature as the deposition (650 °C). RSM was performed after the annealing to confirm that the structural quality of the films is preserved. Finally, the transport properties were again measured under the same conditions as the as-grown films.

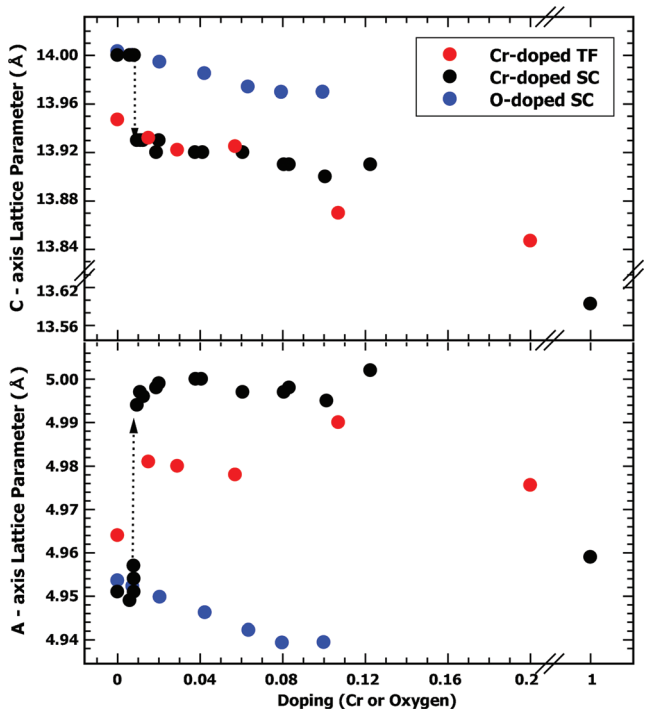

FIG. 2. Lattice parameters as a function of Cr doping of thin films (TF) compared with single crystals (SC). Cr and O-doped SC data extracted from Refs. 19 and 23, respectively.

In order to examine the crystalline quality, the as-grown films were first characterized by high resolution XRD. Figure 1(a) shows $\vartheta/2\vartheta$ scans in logarithmic scale around the symmetric (0006) reflection of the Cr-doped V_2O_3 TF and the Al_2O_3 substrate. Finite size oscillations (Pendellösung fringes) around the layer peak indicate that the films have a smooth surface and interface. The layer peak position shifts from the V_2O_3 to the Cr_2O_3 bulk c lattice parameter when increasing the Cr concentration, confirming the substitutional doping of Cr in the lattice, demonstrated in SC.[17] The absence of extra diffraction peaks indicates that there are no Cr_2O_3 impurities. A RHEED pattern of the undoped sample taken after deposition (Figure 1(b)) presents clear streaks with no indications of poly-crystallinity. RSMs around the (1 0 $\bar{1}$ $\underline{10}$) reflection for the 1.5% Cr-doped sample in Figure 1(c), before and after the annealing, evidence that the films are single phase and that the crystalline quality is preserved after the thermal treatment.

RSMs are also used to extract the lattice parameters of the TF at room temperature, which are shown in Figure 2 and compared with those of SC. It can be seen that indeed, in SC, the effect of Cr and O doping is different. The incorporation of Cr tends to expand the crystalline lattice showing a discontinuous change in the lattice parameters. This is an indication of the PM-PI transition occurring in SC at room temperature when the Cr concentration is varied from 0.8% to 1%.[19] In contrast, for the O-doped SC, the evolution of the lattice parameters shows a smooth decrease with increasing oxygen concentration.[23] Since we grow on Al_2O_3 (lattice parameter $a = 4.754$ Å), an in-plane lattice mismatch will influence the TF. A mismatch of 4.2% and up to 5.2% and 4% are expected for the undoped, Cr and O doping cases, respectively. When comparing TF with Cr-doped SC, it can be

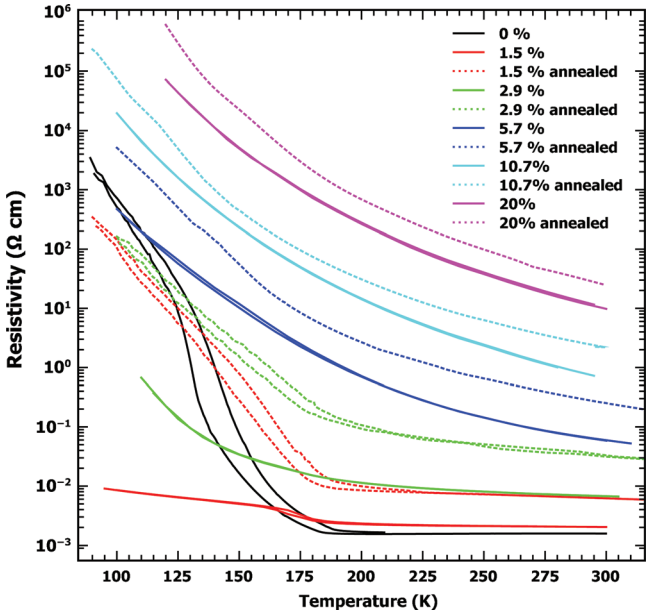

FIG. 3. Resistivity versus temperature of Cr-doped V_2O_3 TF with different Cr concentrations. TF as-grown (continuous line) and after vacuum annealing (dotted line) compared with the undoped V_2O_3 case.

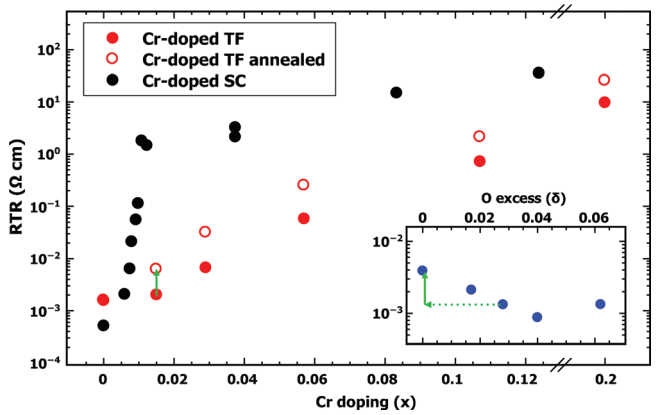

FIG. 4. RTR of Cr-doped SC as a function of doping concentration[19] compared with the as-grown and annealed Cr-doped TF. Inset shows the RTR versus O excess for $V_2O_{3+\delta}$ SC.[23] Vertical green arrows indicate the change in RTR when $\delta = 0.03$ oxygen is removed in SC and the equivalent change in RTR for the 1.5% Cr-doped sample after the annealing.

noted that they are not entirely relaxed. The c-axis value for the undoped film is lower than the bulk value while the a-axis is larger, which arises from the difference in thermal expansion coefficient between the film and the substrate.[15,16] Still the dependence of the c-axis with Cr doping for the TF is in good agreement with the Cr-doped SC, and it can be seen that the values gradually shift towards the Cr_2O_3 bulk value (doping = 1 in the plot). On the other hand, the a-axis lattice parameter remains substantially smaller due to the larger mismatch with the substrate for Cr-doped V_2O_3.

The resistivity versus temperature in the range from 90 K to 300 K of the Cr-doped V_2O_3 TF as-grown and after the vacuum annealing is shown in Figure 3. For the pure V_2O_3 sample, bulk-like electrical properties are found as the sharp and well-known MIT at about 160 K with a resistivity change of 6 decades is clearly observed. In the as-grown case, the resistivity of the samples with higher Cr concentrations (>3%) increases monotonically when decreasing the temperature. However, the sample with 2.9% Cr concentration shows a much lower resistivity compared with higher Cr concentration alloys, and strikingly the one with 1.5% Cr concentration shows a nearly metallic behavior down to 100 K with the consequent suppression of the LT insulating state. Compared to the resistivity of the undoped film at 100 K, this corresponds to a reduction of more than 5 orders of magnitude. What could be the origin of this drastic reduction?

Here, we examine three possibilities to explain the collapse of the LT insulating state. First, it has been reported that hydrogen doping stabilizes a metallic phase in VO_2 thin films.[26,27] However, this type of doping in our Cr-doped samples is very unlikely, since the H_2 partial pressure measured during the use of only the Cr cell is one order of magnitude smaller than the one originated by the V source. The second possibility is the effect of disorder as recently reported for irradiated V_2O_3 TF.[28] However, in our case, the high temperature growth process leads to bulk-like (structural and electrical) properties in pure V_2O_3 TF suggesting limited disorder in our films.[16] Finally, the third option is the addition of oxygen that changes the electrical properties of V_2O_3 towards the metallic state at low temperatures.[22–24] This effect has also been observed in low Cr-doped SC.[25] Hence, we propose that Cr doping promotes oxygen excess in our films during deposition, leading to the collapse of the LT insulating state at low Cr concentrations.

To confirm this hypothesis, the Cr-doped V_2O_3 TF were annealed in vacuum for 5 min at the same temperature as the deposition temperature. We can observe in Figure 3 that the transport properties of the low Cr-doped samples have changed significantly upon annealing. The observed large increase in the LTR—almost up to the value of the undoped case—and the presence of hysteresis, both confirm that the LT insulating state and the MIT have been recovered for the 1.5% Cr-doped film. Meanwhile, for the higher Cr-doped samples after annealing, a shift towards higher resistivities for the entire curve is observed.

In Figure 4, the RTR for different Cr doping concentrations in SC is compared with the corresponding values for the TF in the as-grown as well as in the annealed state. Again, we observe that Cr doping is different from O doping in bulk, the RTR increases about four orders of magnitude with the insertion of only 1% Cr[19] while moderate O doping (see inset) has the opposite effect, the RTR gradually decreases as the system becomes more metallic.[23] In our films, the RTR is much more reduced than the bulk case, partially due to strain that most likely hinders the PM-PI transition to occur. After annealing in vacuum, we observe an increase of RTR in all the TF alloys evolving towards the bulk case. It is important to notice that for the undoped film there is no change in RTR after the annealing—the data points in the figure overlap completely—which is consistent with stoichiometric V_2O_3 films. Furthermore, for the lowest Cr concentration, the change in RTR is about 3×10^{-3} Ω cm, which is nearly the same as the one upon removal of 0.03 oxygen excess in non-stoichiometric SC.[23] These

changes are indicated with the vertical green arrows in the figure. Hence, we can estimate that the amount of oxygen lost during the annealing—for the lowest Cr-doped sample—corresponds to about 1%.

When Cr doping is added, the 24% increment (from 4.2% to 5.2%) in the in-plane lattice mismatch with the substrate needs also to be accommodated by the TF. The insertion of oxygen would thus lead to a smaller mismatch and can explain its preferential incorporation when Cr-doped TF are grown. There are two other mechanisms which can contribute to an increase of the oxygen content in Cr-doped films: (1) the larger electron affinity of Cr atoms in comparison with V atoms; (2) the increased average lattice spacing of Cr-doped films allows more oxygen atoms to be incorporated during growth. This additional oxygen (or cation vacancies) is later removed by the vacuum annealing at high temperature.

However, after the annealing, the properties both structurally as well as electrically do not yet reach those of the equivalent bulk compounds. In SC, the change in lattice parameter (see Figure 2) across the PM–PI transition can account at least partially for the resistivity jump across the transition. The a lattice parameter as well as the lattice volume $= a^2c \sin(60°)$ both increase by about 1%, which leads to a reduction of the orbital overlap and thus a decrease of bandwidth (or, equivalently, a strengthening of the electron correlations). Note that the change in lattice parameters in our films after the annealing is very small (less than 0.05%, not shown here). Therefore, the absence of this transition even after the vacuum annealing may be attributed to the large in-plane mismatch and the clamping to the substrate, which prevents the in-plane lattice parameter to change in the TF as it is observed in bulk.[19] In a previous work,[16] it has been shown that the MIT in V_2O_3 layers grown directly on Al_2O_3 is lost for thicknesses below 5 nm due to the presence of a large strain; however, the transition can be recovered when a thin Cr_2O_3 buffer layer is inserted. Then, the growth of TF alloys on substrates with a larger in-plane lattice parameter may help to further understand the present results.

In conclusion, we demonstrate that high quality Cr-doped V_2O_3 TF can be grown epitaxially. We report structural and electrical properties of TF alloys with Cr concentrations up to 20% grown by MBE. For the highly doped samples (>3%), an increase of the resistance with decreasing temperature is measured. Strikingly, for the low doped samples (<3%), a collapse of the insulating state is observed with a reduction of the low temperature resistivity by up to 5 orders of magnitude. Using a vacuum annealing procedure at high temperature, the LT insulating state is recovered for these films showing evidence that an oxygen excess introduced during the film growth is responsible for the observed collapse. Therefore, our results also demonstrate that co-doping with Cr as well as with O is possible in TF. This gives to the V_2O_3 system *two handles working in opposite directions*. Furthermore, since oxygen can be mobile under the application of an electric field,[9,29,30] these results suggest that the Cr-O-V system holds a great potential for different electronic devices. Moreover, it will be interesting to investigate the resistive switching behavior in our films in vertical Cr-doped V_2O_3 based structures and in different environments as well.

The authors acknowledge financial support from the FWO Project No. G052010N10 as well as the EU-FP7 SITOGA Project. P.H. acknowledges support from Becas Chile—CONICYT.

[1]H. A. Wriedt, Bull. Alloy Phase Diagrams **10**, 271 (1989).
[2]U. Schwingenschlögl and V. Eyert, Ann. Phys. **13**, 475 (2004).
[3]D. McWhan, A. Menth, J. Remeika, W. Brinkman, and T. Rice, Phys. Rev. B **7**, 1920 (1973).
[4]F. J. Morin, Phys. Rev. Lett. **3**, 34 (1959).
[5]Z. Yang, C. Ko, and S. Ramanathan, Annu. Rev. Mater. Res. **41**, 337 (2011).
[6]S. Guenon, S. Scharinger, S. Wang, J. G. Ramirez, D. Koelle, R. Kleiner, and I. K. Schuller, Europhys. Lett. **101**, 57003 (2013).
[7]J. S. Brockman, L. Gao, B. Hughes, C. T. Rettner, M. G. Samant, K. P. Roche, and S. S. P. Parkin, Nat. Nanotechnol. **9**, 453 (2014).
[8]C. Ko and S. Ramanathan, Appl. Phys. Lett. **93**, 252101 (2008).
[9]J. Jeong, N. Aetukuri, T. Graf, T. D. Schladt, M. G. Samant, and S. S. P. Parkin, Science **339**, 1402 (2013).
[10]H. Madan, M. Jerry, A. Pogrebnyakov, T. Mayer, and S. Datta, ACS Nano **9**, 2009 (2015).
[11]H. Schuler, S. Klimm, G. Weissmann, C. Renner, and S. Horn, Thin Solid Films **299**, 119 (1997).
[12]Q. Luo, Q. Guo, and E. G. Wang, Appl. Phys. Lett. **84**, 2337 (2004).
[13]S. Yonezawa, Y. Muraoka, Y. Ueda, and Z. Hiroi, Solid State Commun. **129**, 245 (2004).
[14]S. Autier-Laurent, B. Mercey, D. Chippaux, P. Limelette, and Ch. Simon, Phys. Rev. B **74**, 195109 (2006).
[15]L. Dillemans, R. R. Lieten, M. Menghini, T. Smets, J. W. Seo, and J. P. Locquet, Thin Solid Films **520**, 4730 (2012).
[16]L. Dillemans, T. Smets, R. R. Lieten, M. Menghini, C.-Y. Su, and J.-P. Locquet, Appl. Phys. Lett. **104**, 071902 (2014).
[17]A. I. Frenkel, D. M. Pease, J. I. Budnick, P. Metcalf, E. A. Stern, P. Shanthakumar, and T. Huang, Phys. Rev. Lett. **97**, 195502 (2006).
[18]A. Jayaraman, D. B. McWhan, J. P. Remeika, and P. D. Dernier, Phys. Rev. B **2**, 3751 (1970).
[19]D. B. McWhan and J. P. Remeika, Phys. Rev. B **2**, 3734 (1970).
[20]H. Kuwamoto, J. M. Honig, and J. Appel, Phys. Rev. B **22**, 2626 (1980).
[21]P. A. Metcalf, S. Guha, L. P. Gonzalez, J. O. Barnes, E. B. Slamovich, and J. M. Honig, Thin Solid Films **515**, 3421 (2007).
[22]D. B. McWhan, A. Menth, and J. P. Remeika, J. Phys. (Paris) **32**, C1-1079 (1971).
[23]Y. Ueda, K. Kosuge, and S. Kachi, J. Solid State Chem. **31**, 171 (1980).
[24]S. A. Shivashankar and J. M. Honig, Phys. Rev. B **28**, 5695 (1983).
[25]H. Kuwamoto and J. M. Honig, J. Solid State Chem. **32**, 335 (1980).
[26]C. Wu, F. Feng, J. Feng, J. Dai, L. Peng, J. Zhao, J. Yang, C. Si, Z. Wu, and Y. Xie, J. Am. Chem. Soc. **133**, 13798 (2011).
[27]Y. Zhao, G. Karaoglan-Bebek, X. Pan, M. Holtz, A. A. Bernussi, and Z. Fan, Appl. Phys. Lett. **104**, 241901 (2014).
[28]J. G. Ramirez, T. Saerbeck, S. Wang, J. Trastoy, M. Malnou, J. Lesueur, J.-P. Crocombette, J. E. Villegas, and I. K. Schuller, Phys. Rev. B **91**, 205123 (2015).
[29]M. Quintero, P. Levy, A. G. Leyva, and M. J. Rozenberg, Phys. Rev. Lett. **98**, 116601 (2007).
[30]C. Yoshida, K. Kinoshita, T. Yamasaki, and Y. Sugiyama, Appl. Phys. Lett. **93**, 042106 (2008).